Light scattering from quantum confined and interface optical vibrational modes in strained-layer GaSb/AlSb superlattices

G. P. Schwartz, G. J. Gualtieri, and W. A. Sunder
AT&T Bell Laboratories, Murray Hill, New Jersey 07974-2070

L. A. Farrow
Bell Communications Research, Red Bank, New Jersey 07701-7020
(Received 4 February 1987)

Raman scattering has been performed on GaSb/AlSb strained-layer superlattices with periods varying from 65 to 300 Å. Discrete quantum confined GaSb longitudinal optical phonons are observed in GaSb layers less than 25 Å thick. The confinement-induced Γ-to-L crossover in GaSb manifests itself in our spectra via the observation of optical-phonon density-of-states structure. This structure disappears for GaSb layers thicker than 50 Å. Spatially extended interface modes have been observed in all superlattices in both the GaSb and AlSb optical-mode spectra.

I. INTRODUCTION

A number of studies[1–10] have treated both the theoretical and experimental aspects of optical phonons propagating along the growth axis in superlattice structures. If the optical-phonon density of states in the two materials do not overlap in frequency, as occurs in GaAs/AlAs or GaSb/AlSb couples, then the bulk optical modes are confined within their respective layers and the mode frequencies are expected to exhibit quantum confinement effects as the layer widths are decreased. These modes are similar to the resonance vibrations of isolated slabs[11] with the caveat that the mechanical boundary conditions at the interfaces are modified due to the presence of the bounding dielectric layers, and as a consequence, the allowed quantized wave vector in an individual superlattice layer differs somewhat from that of an isolated slab.[12,13] In addition to the confined slab modes with wave vectors quantized along the superlattice growth axis, there exist interface vibrational modes which propagate in the plane of the individual layers.[14–17] The potential associated with these localized modes extends across their respective interfaces, producing coupled vibrations which are described as "spatially extended" along the superlattice growth axis.

Most experimental studies have focussed on nearly lattice-matched GaAs/(Al,Ga)As superlattices. For pseudomorphic growth of lattice-mismatched superlattices, the growth axis is subject to a tetragonal distortion and in-plane strain exists throughout the structure. The effect of these parameters on the lattice dynamics of confined and interfacial optical modes have received little attention to date. In the present work, confined and interface optical phonons have been examined in GaSb/AlSb superlattices which exhibit a room-temperature lattice mismatch of 0.65%.

II. EXPERIMENT

The superlattice samples were grown on (001) or (111) GaSb substrates at temperatures between 490 and 505 °C by molecular beam epitaxy. The nominal growth period was refined by measuring the frequencies of folded acoustic longitudinal modes and matching these frequencies to elastic continuum-model calculations.[18] Table I provides a compilation of the samples including their substrate orientation, buffer layer composition, the total number of periods in the superlattice, the refined value of the period, and the total superlattice thicknesses. In all cases the superlattices were terminated with GaSb due to the reactivity of AlSb with moist air.

Raman spectra were collected with use of the 5145-Å excitation in a Brewster's-angle surface reflection geometry. The Raman scattered light was analyzed using a 1-m double-pass spectrometer equipped with holographic gratings. The samples were mounted in an evacuated Dewar and measurements were made at room and liquid-nitrogen temperatures. For scattering from (001) surfaces the axes are defined as follows: $x(100)$, $y(010)$, $z(001)$, $x'(110)$, and $y'(1\bar{1}0)$. For scattering from (111) substrates the axes are defined as $z''(111)$, $x''(1\bar{1}0)$, and $y''(11\bar{2})$. Standard scattering notation is employed, i.e., $z(x,y)\bar{z}$ represents light incident along z and polarized along x, with the scattered light emitted along $\bar{z}$ and polarized along y. The instrumental resolution varied between 1.4 and 3 cm^{-1} depending upon which region of the spectrum was being examined.

III. RESULTS AND DISCUSSION

A. Quantum confined optical phonons

The spatial confinement of optical phonons in bilayer superlattice structures is a manifestation of the damping which occurs when the optical-phonon densities of states in a particular propagation direction do not overlap for the two constituent materials. This is illustrated in Fig. 1, where the real and imaginary components of the phonon wave vector for bulk GaSb and AlSb have been plotted based on linear-chain model calculations employing the dispersion equation

TABLE I. Samples grown on GaSb substrates.

Sample	Substrate orientation	Buffer	Number of periods (N)	d (Å)	Nd (Å)
1	(001)	GaSb	20	200	4000
2	(001)	GaSb	20	187	3740
3	(001)	GaSb	12	203	2436
4	(001)	GaSb	20	300	6000
5	(001)	GaSb	20	130	2600
6	(001)	GaSb	34	64.8	2203
7	(001)	GaSb	15	61.9	929
8	(001)	AlSb	15	63.5	953
9	(111)	GaSb	15	74.5	1118
10	(001)	GaSb	15	71.4	1071
11	(001)	GaSb	15	68.0	1020

$$\cos(q\alpha)=\frac{(M_1\omega^2-2K)(M_2\omega^2-2K)-2K^2}{2K^2} . \quad (1)$$

In this expression, M_1 and M_2 denote the two masses in the unit cell, K the force constant, and α the lattice constant of the chain, i.e., half the cubic lattice constant a. We denote the component of the wave vector along the superlattice growth axis by q; the in-plane component will be called k.

Both materials have purely imaginary wave vectors in the range of optical frequencies exhibited by their complementary component. A zone-center GaSb phonon experiences $1/e$ damping of its amplitude after propagating ~ 0.6 monolayers (1.8 Å) into AlSb, whereas phonons at the AlSb zone-center frequency are attenuated nearly three times as rapidly when propagating in GaSb. As a consequence, longitudinal-optical (LO) phonons propagating along the (001) superlattice growth axis are best described as confined and exhibit standing wave character. In this respect they resemble confined slab modes,[11] whose wave vectors are quantized in units of $m\pi/(n\alpha)$, where $n\alpha$ is the width of the phonon well in monolayers. Since the slabs are bounded rather than isolated in a superlattice structure, the mechanical boundary condition on the amplitude of vibration of the interface atom is relaxed.[12,13] In the limit of an infinitely short decay length, the wave vector quantization condition becomes[13] $k=m\pi/(n+1)\alpha$. For finite decay lengths, the factor $(n+1)$ must be replaced with a value which lies between n and $n+1$.

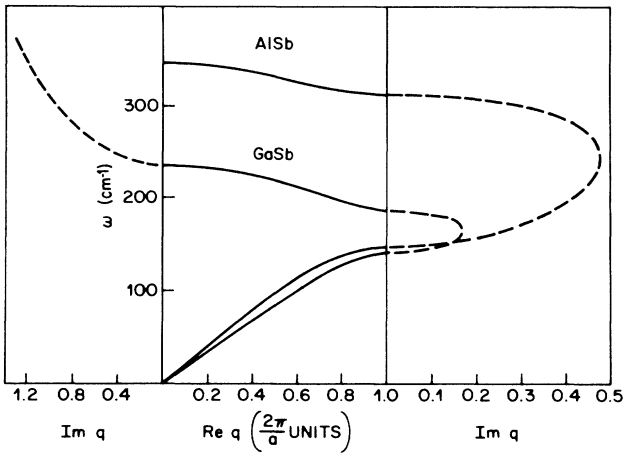

FIG. 1. Complex longitudinal-phonon dispersion curves $\omega(q)$ for GaSb and AlSb for propagation along (001) computed using the linear-chain model. The values used for the force constants were 0.7126×10^5 dyn/cm^2 and 0.7706×10^5 dyn/cm^2 for GaSb and AlSb, respectively, corresponding to LO frequencies of 233.6 and 339.6 cm^{-1}.

Resolved quantized LO phonons have previously been observed[7,9,10,19,20] in nearly lattice-matched superlattices with individual layers of order 25–30 Å, or equivalently 10 monolayers. The peaks are generally labeled with the index m according to the symmetry of their vibrational amplitudes[11]

$$U_m \propto \cos(m\pi z/d_1), \quad m=1,3,5,\ldots \quad (2)$$

$$U_m \propto \sin(m\pi z/d_1), \quad m=2,4,6,\ldots \quad (3)$$

in which the origin is taken to be the center of the slab of thickness d_1. The quantized frequencies LO_m are nearly dispersionless since the dispersion is related to the ratio of the decay length to the barrier width.[2]

The LO vibrations along the superlattice axis belong either to the B_2 (m odd) or A_1 (m even) representations of the D_{2d} point group. For off-resonance scattering, the B_2 symmetry phonons should be Raman active in the (x,y) and (x',x') configurations, whereas the A_1 phonons will be active in (x,x) and (x',x'). These selection rules no longer hold if the excitation frequency is in resonance with the excitonic levels of the quantum well.[9] In principle, the (x',x') scattering configuration contains contributions from both B_2 and A_1 symmetry phonons. Bond polarizability calculations for GaAs/(Ga,Al)As superlattices suggest however, that for off-resonance scattering the Raman cross section for A_1 symmetry phonons will be much smaller than that for B_2 symmetry phonons.[20] The latter prediction has been verified by a number of authors working with GaAs/(Ga,Al)As superlattices. In Refs. 7 and 20 the A_1 symmetry (m even) phonons were not detected at all, whereas in Refs. 10 and 19 they were, but with reduced scattering strength.

The anticipated polarization and scattering intensity

predictions of theory are borne out in our data illustrated in Fig. 2 for scattering at 77 K from a superlattice (sample 11) with a nominal GaSb layer width of 12.2 Å or 4 monolayers. The even- and odd-m LO phonons are separated in the (x,y) and (x,x) configurations. In the (x',x') configuration, the relative strengths of LO_1 and LO_3 compared to their (x,y) configuration counterparts suggest the presence of both A_1 and B_2 phonons which are not individually resolved. Neither even- nor odd-m LO phonons are allowed in (x',y'); the residual signal which is observed represents polarization leakage and relaxation of the symmetry selection rule which makes TO (E representation) scattering forbidden from the (001) orientation. The structures labeled IF and $S1$ denote interface mode and large wave-vector scattering processes whose properties will be examined in Secs. IV B and IV C, respectively.

At room temperature, thermal broadening generally precludes the resolution of quantum confined optical phonons other than LO_1 and LO_2 (see Fig. 3). The interface mode is more intense (relative to LO_1) at 300 K, but the additional structure labeled $S1$ in Fig. 2 is now absent. We have also noted that in the (x',y') scattering configuration, the selection rules for the LO_m phonons are more rigorously obeyed at 300 K than at 77 K. This probably reflects weak "near resonance" contributions to the scattering since the excitation energy (2.4 eV) lies close to a number of fundamental transitions including the E_0 (2.38 eV) and E_L (2.33 eV) gaps in AlSb and the E_1 (2.19 eV) and $E_1+\Delta_1$ (2.62 eV) transitions in GaSb (Ref. 21) (all data are for 27 K).

The observed confined phonon frequencies at 77 K (ω_{LN}), their polarization character, and two calculations of the quantized wave vector q_a and q_b are presented in Table II. The wave vectors were calculated from $q_a = m\pi/d_1$, where d_1 is the GaSb layer width, and $q_b = m\pi/(n+1)\alpha$, where n is the nominal number of integral monolayers and $\alpha = 3.048$ Å. Both q_a and q_b have been normalized to the Brillouin zone width in Table II. Frequencies at 300 K (ω_{RT}) were obtained by applying a 3.3 cm^{-1} correction to ω_{LN} in order to facili-

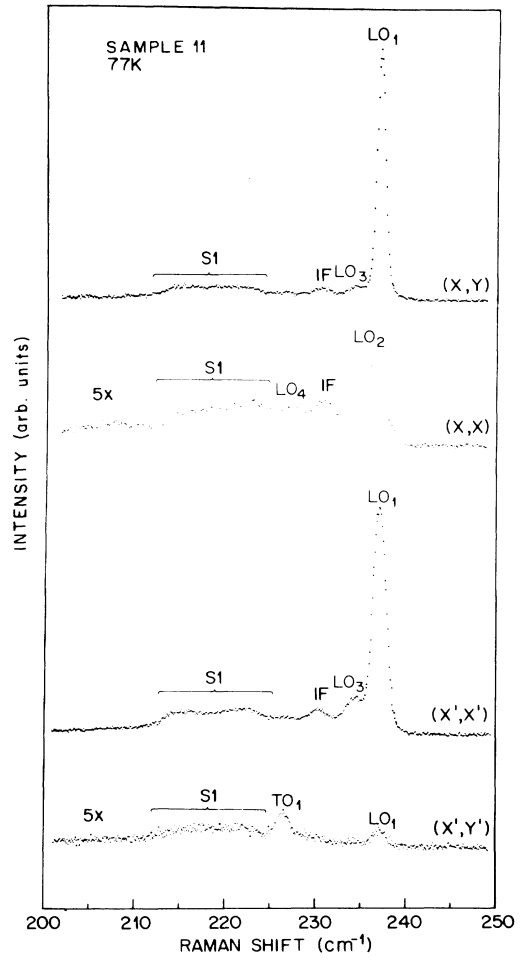

FIG. 2. Raman scattering polarization dependence of the quantized GaSb LO phonon modes labeled by LO_m at 77 K. The designation IF refers to an interface mode. The structure denoted by $S1$ is discussed in Sec. III C and is not directly related to the observation of quantized optical phonons.

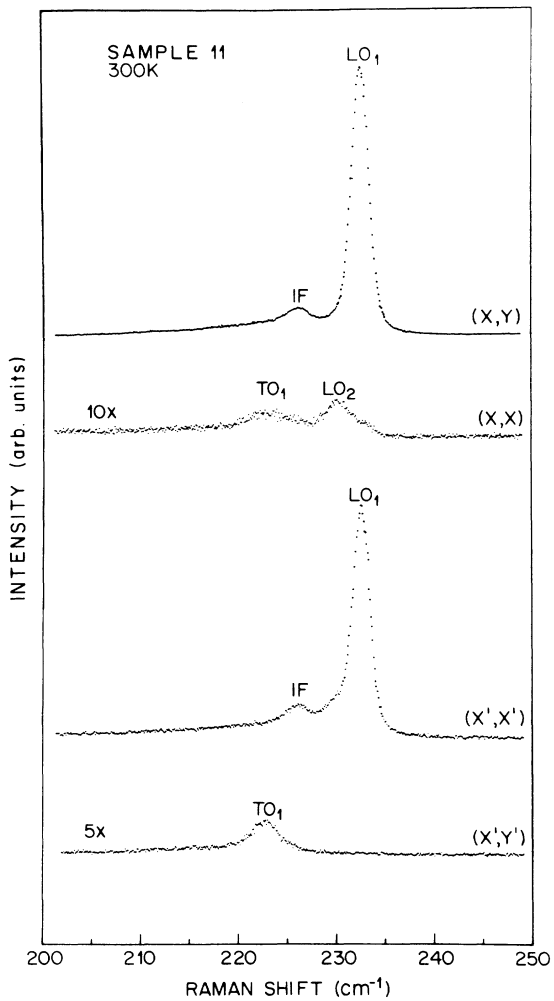

FIG. 3. Polarization dependence of the room-temperature Raman spectrum in the frequency range for GaSb optical phonons. The peak labeled IF is discussed in the text.

TABLE II. Quantum confined optical-phonon frequencies in GaSb/AlSb superlattices.

Mode	Sample	Polarization	ω_{LN} (cm^{-1})	ω_{RT} (cm^{-1})	d_1 (Å)	n (ml)	q_a	q_b
LO_1	11	(x',x')	236.4	233.1	13.1	4	0.233	0.200
	11	(x,y)	237.0	233.7	13.1	4	0.233	0.200
	8	(x,y)	236.9	233.6	24.1	8	0.126	0.111
LO_3	11	(x',x')	233.8	230.5	13.1	4	0.698	0.600
	11	(x,y)	234.2	230.9	13.1	4	0.698	0.600
	8	(x,y)	235.1	231.8	24.1	8	0.379	0.333
LO_5	8	(x,y)	229.8	226.5	24.1	8	0.632	0.555
LO_2	11	(x,x)	235.1	231.8	13.1	4	0.465	0.400
	8	(x,x)	236.0	232.7	24.1	8	0.253	0.222
LO_4	11	(x,x)	227.2	223.9	13.1	4	0.931	0.800
	8	(x,x)	231.1	227.8	24.1	8	0.506	0.444

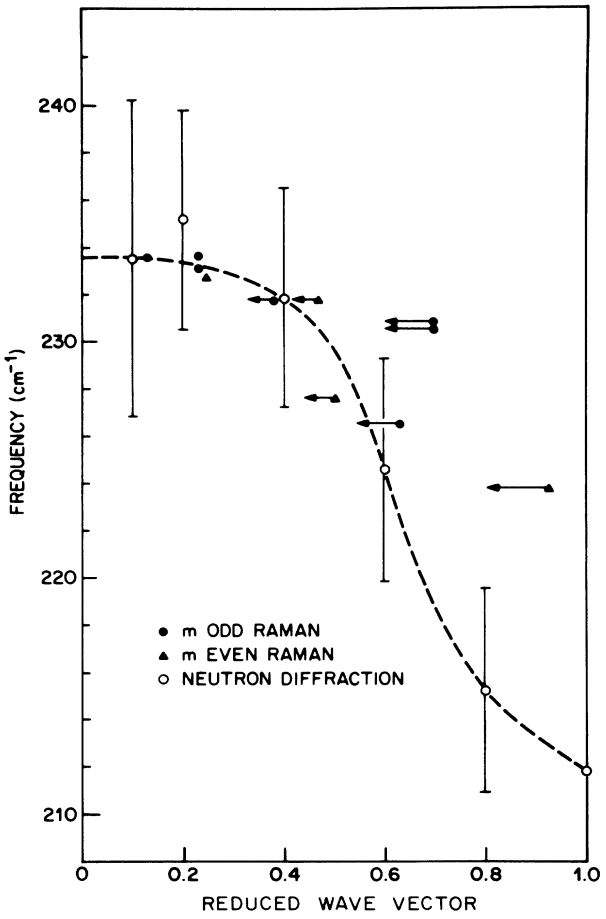

FIG. 4. Bulk (neutron diffraction) and quantized (solid symbols) GaSb LO phonon frequencies plotted against the reduced wave vector for phonon propagation along (001). The dashed curve is a visual fit to the neutron data. The arrows connected to the solid symbols represent the size of corrections associated with the choice of mechanical boundary conditions on the slab mode solutions.

tate comparison with the room-temperature neutron diffraction data of Farr *et al.*[22] This comparison is presented in Fig. 4, in which the arrows attached to the Raman data indicate the width spanned by q_a and q_b. For small q values ($q < 0.25$), the arrows have been omitted from Fig. 4 because they are too short to distinguish clearly.

One of the current issues in superlattice optical-phonon studies concerns the question of whether the confined LO phonons consistently lie at higher frequencies than the bulk dispersion curves for large reduced wave-vector values ($q > 0.6$). Both points of view are represented in the literature.[13,23] The bulk dispersion curves are normally taken from neutron diffraction data. The tabulated neutron diffraction data of Ref. 22 are shown plotted along with a dashed curve which we have visually drawn through the available points (Fig. 4). The neutron data have not been shifted relative to the tabulated values because the extrapolated GaSb LO frequency comes close to the value of 233.6 cm^{-1} which we routinely observe at 300 K in Raman scattering. We note, however, that the same tabulation gives a transverse-optical (TO) frequency of $\sim$229 cm^{-1}, which we consider to be too large by 5–6 cm^{-1}. On the other hand, the neutron measurement at the (100) zone boundary ($\sim$212 cm^{-1}) is only 2 cm^{-1} higher than the value reported using overtone Raman scattering.[24] The necessity for applying a uniform shift to the neutron diffraction data is questionable in view of the errors quoted in Ref. 22, which range from ± 4.3–6.7 cm^{-1}.

Examination of Fig. 4 would suggest that quantum confined GaSb LO phonons appear at higher than bulk frequencies for large wave vectors, even allowing for the shift entailed by using the appropriate mechanical boundary conditions. The latter assertion should be viewed critically within the context of possible experimental errors. Primary among these errors are (1) the possibility of erring in the assignment of the LO_4 phonon in the $z(x,x)\bar{z}$ spectrum of sample 11, (2) uncertainties in the width d_1 of the GaSb layer, and (3) errors in mea-

surement of the peak frequencies.

The peak frequencies can easily be measured within ± 0.3 cm^{-1}. In addition, there will be small shifts due to the biaxial tension (GaSb) or compression (AlSb) in the respective layers due to the lattice mismatch. Biaxial tension in the GaSb would shift the observed frequencies down,[25] which would shift the data toward rather than away from the bulk dispersion curve. For growth on GaSb substrates or thick GaSb buffer layers, the strain in the GaSb layer should in fact be small, and we typically observe strain-related downshifts of the GaSb frequencies of less than 0.3 cm^{-1}.

Excursions in the superlattice period $d = d_1 + d_2$ have been checked by measuring the folded acoustic mode spectrum for each sample and fitting the peak positions to the elastic continuum model.[26] For superlattice samples 8 and 11 the folded mode periods were 98% and 105% of the nominal period predicted by calibrated growth rate measurements.[18] The GaSb layer width d_1 listed in Table II reflects the expansion (sample 11) or contraction (sample 8) of the overall period based on these measurements.

The assignment of the LO_4 phonon in sample 11 is clearly critical to making a strong case for the confined LO modes lying above the bulk frequencies. Unfortunately, the frequency of the LO_4 phonon is nearly coincident with the symmetry forbidden TO phonon. If one removes this data point from Fig. 4, there is no clear resolution as to the agreement of confined and bulk LO phonon frequencies, particularly in view of the large experimental error bars on the neutron diffraction data. For large values of m, the presence of the structure $S1$ further complicates the ability to resolve the confined phonon peaks unambiguously.

B. Optical interface modes

In isolated slabs the normal modes of vibration include surface modes in addition to standing-wave slab resonances.[27] In a superlattice with finite layer thicknesses d_1 and d_2, the electric fields associated with the surface vibrations overlap, producing coupled interface modes which represent collective excitations of the superlattice structure.[14,15,28,29] The dispersion relation derived from an analysis of Maxwell's equations is given by

$$\cos(qd) = [(\eta^2+1)/2\eta]\sinh(kd_1)\sinh(kd_2) + \cosh(kd_1)\cosh(kd_2)\ , \tag{4}$$

where $\eta \equiv \epsilon^A(\omega)/\epsilon^B(\omega)$, with ϵ^A and ϵ^B representing the dielectric constants of the superlattice constituents GaSb and AlSb, and d_1 and d_2 are their respective layer widths. The quantities q and k are the components of the wave vector perpendicular (growth axis) and parallel to the layers. In the infrared region where the frequency-dependent dielectric constant is given by

$$\epsilon(\omega) = \epsilon_\infty + \frac{\omega_{TO}^2(\epsilon_0 - \epsilon_\infty)}{(\omega_{TO}^2 - \omega^2)}\ , \tag{5}$$

there exist four real roots to Eq. (4) bounded in pairs between the LO-TO spectral ranges of the two materials constituting the superlattice. The interface modes lying between the LO and TO of GaSb will be denoted as "GaSb-like," and those between the LO and TO of AlSb as "AlSb-like." The electrostatic potential associated with these modes has symmetric and antisymmetric components relative to an origin placed at the center of a slab, which are denoted as + and −, respectively, for $d_1 < d_2$ with the origin located at the center of a GaSb layer.

Representative data for the temperature and polarization dependence of the GaSb-like and AlSb-like interface modes are shown in Figs. 2, 3, 5, and 6 for sample 11 (period 68 Å). The peak labeled $S2$ lies outside the allowed frequency regime for interface modes and will be discussed in Sec. III C. A compendium of observed interface mode frequencies is given in Table III. An interesting division exists between short-period ($d \leq 75$ Å) and long-period (130 Å $\leq d \leq$ 300 Å) structures. In all

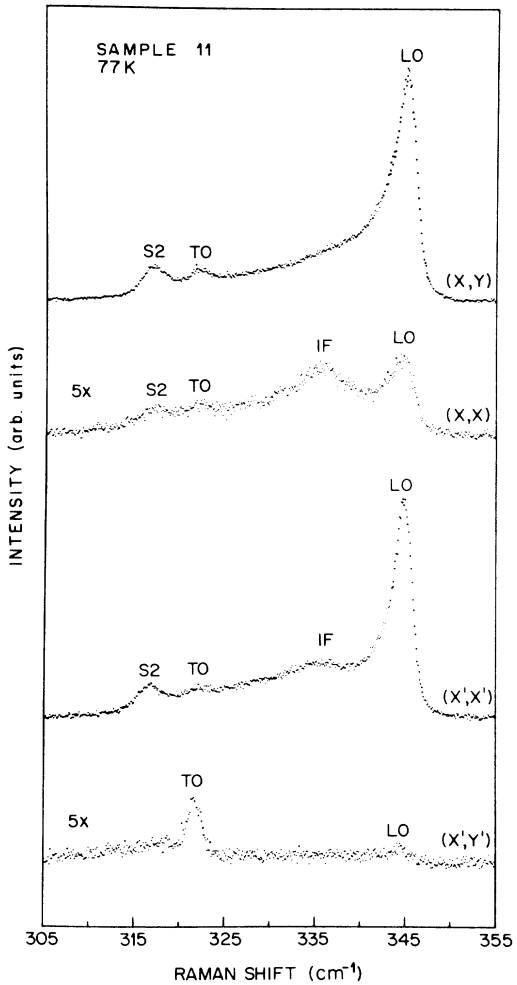

FIG. 5. Polarization dependence of the 77 K Raman scattering in the frequency regime of AlSb optical phonons. The interface mode (IF) is seen most clearly in the (x,x) scattering configuration. The structure labeled $S2$ is discussed in Sec. III C of the text.

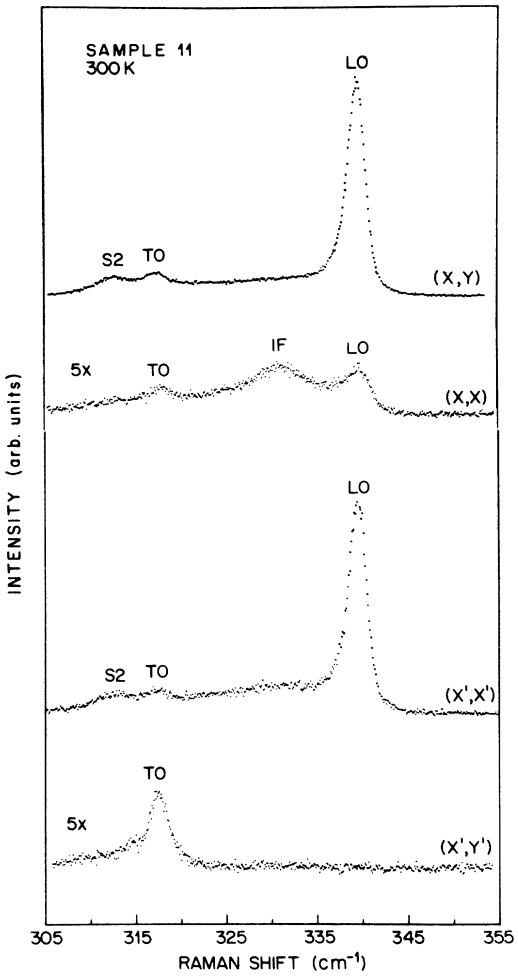

FIG. 6. Room-temperature polarized Raman scattering in the vicinity of the AlSb LO and TO phonons for sample 11.

cases, $d_1(\text{GaSb}) < d_2(\text{AlSb})$. A synopsis of observations for the two divisions includes the following.

1. $d \leq 75$ Å

In short-period structures a moderately narrow (3–5 cm^{-1}) GaSb-like interface mode is detected between 4.8 and 6.6 cm^{-1} below the GaSb LO (or LO_1 in samples exhibiting confinement), whereas a relatively broad (10–12 cm^{-1}) AlSb-like interface mode is observed 8.2–9.6 cm^{-1} below the AlSb LO frequency. The single exception is sample 9 which was grown on a (111)-oriented substrate. Raman scattering at 77 K is shown in Fig. 7 for that wafer. The interface (IF) mode frequencies are the same (within 0.5 cm^{-1}) at 77 and 300 K. The GaSb-like IF mode is strong in either the (x,y) or (x',x') scattering configuration, weak but distinguishable in (x,x), and absent in (x',y'). Although the integrated intensity of the AlSb-like mode is large in the (x,y) and (x',x') configurations, it is often not possible to assign a peak position due to its width. The peak can be located in the (x,x) configuration however, whereas it is totally extinguished in (x',y'). Qualitatively, the GaSb-like IF mode is strong at 300 K and somewhat weaker at 77 K, whereas the opposite obtains for the AlSb-like interface mode.

2. 130 Å $\leq d \leq$ 300 Å

In long-period structures, the GaSb-like interface mode is no longer observed as a distinct peak even at 77 K; instead it manifests as a shoulder on the GaSb LO peak. We have noted that even in the (x,x) scattering configuration, the rejection of the B_2 symmetry LO phonon is much less complete than what was observed in short-period samples. This artifact may be associated with the nucleation of misfit dislocations, which occur

TABLE III. Interface phonon frequencies at 77 K.

Sample	$\omega_{LO}-\omega_{IF}$ (cm^{-1}) GaSb	AlSb	d_1 (Å)	d_2 (Å)	qd	kd
11	6.6	9.1	13.1	54.9	0.68	0.05
10	6.1	9.7	31.2	40.2	0.71	0.06
8	4.6	9.6	24.1	39.4	0.64	0.05
7	5.9	8.8	23.4	38.5	0.62	0.05
6	4.8	13.5, ~8.2[a]	26.6	38.2	0.65	0.05
9[b]	~2–3	6.2	28.3	46.2	0.75	0.06
1[c]	shoulder (LO)	13.7	50	150	2.0	0.16
2	shoulder (LO)	13.3	53.4	133.6	1.9	0.15
3	shoulder (LO)	14.7	103	100	2.0	0.16
4[c]	shoulder (LO)	15.1	50	250	3.0	0.24
5[c]	shoulder (LO)	15.0	50	80	1.3	0.10

[a] Discernable two peak structure.
[b] (111) substrate orientation.
[c] Period estimated from nominal growth rates.

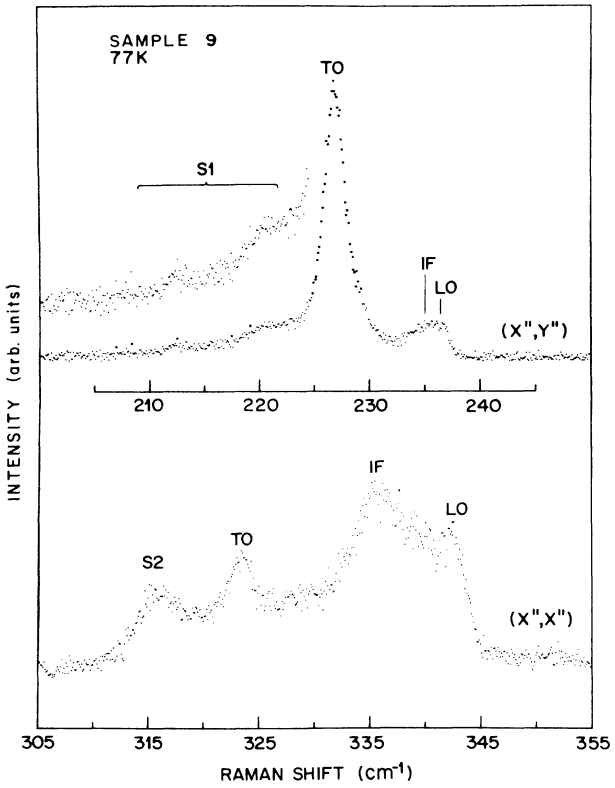

FIG. 7. Two specific polarizations for Raman scattering at 77 K from the optical-phonon regions of GaSb (upper) and AlSb (lower) for the (111)-oriented sample 9.

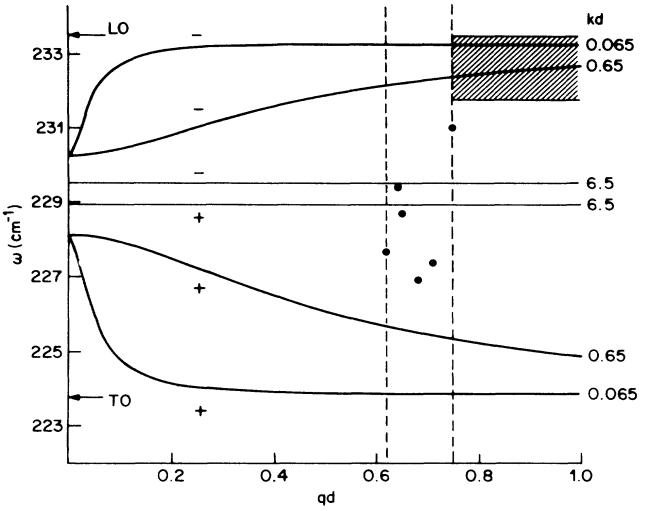

FIG. 8. Calculated (solid lines) and experimentally observed (solid circles) GaSb-like optical interface-mode frequencies plotted as a function of the growth axis wave vector q for various values of the in-plane wave vector k, where d is the superlattice period. The designations + and − label the symmetry of the potential with respect to the center of a GaSb slab. The vertical dashed lines delineate the qd boundaries of the short-period samples. The shaded region bounds the frequency limits for interface modes found in long-period samples; the actual data lies outside of the qd limits on this plot.

when the total GaSb/AlSb superlattice thickness exceeds some 2000 Å.[30] Due to the strong residual LO signal in (x,x) and the closeness of the peak to the LO frequency, we can only estimate that for the GaSb-like IF mode (LO-IF)~ 2 cm^{-1}. The AlSb-like interface mode is discernible however, although it is again 10–12 cm^{-1} broad. In the long-period superlattices, this interface mode is now shifted to a position lying between 13.3 to 15.1 cm^{-1} below the AlSb LO frequency.

Figures 8 and 9 show the calculated GaSb-like and AlSb-like interface-mode frequencies as a function of qd for various values of the in-plane parameter kd. The observed IF mode frequencies for the short-period superlattices are shown as solid circles, whereas the range of frequencies measured in long-period structures is denoted by a shaded band since the data lie outside the qd range of the figures.

In the surface-reflection backscattering geometry employed in these experiments, q is $\sim 1.0\times 10^6$ cm^{-1} and $k\sim 0.8\times 10^5$ cm^{-1}. The observed frequencies are in poor agreement with the calculated curves using these parameters. Abnormally large values of k are required in the calculations in order to obtain the observed interface-mode frequencies. The only apparent exception to this is the GaSb-like interface mode in the long-period structures. Note that in the samples with $d<75$ Å, the observed peaks lie in the frequency regime where the electrostatic potential has symmetric (+) character, whereas for $d>130$ Å, the interface modes are found in the half-plane where the potential has antisymmetric (−) character. (The data point for sample 9 is an exception.) It should be borne in mind that $d_1<d_2$ for both the long- and short-period structures, so that the inversion of the half-plane zone in which the IF mode peak is observed cannot be explained on that basis.

Although the scatter is fairly large, the data tend to group around the frequencies predicted by the long-wavelength limit[5] ($q\rightarrow 0$). It is clear however, that the calculated curves show strong dispersion for finite q

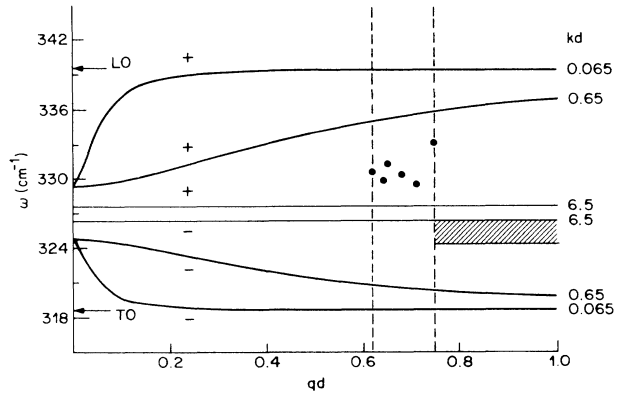

FIG. 9. Calculated (solid lines) and experimental (solid symbols) AlSb-like optical interface-mode frequencies. The labeling is the same as in Fig. 8.

when k is small, and it is difficult to justify using the long-wavelength limit in our experimental configuration. The discrepancy between the in-plane k values estimated from the scattering geometry and those needed to achieve agreement with the measured frequencies suggested that we should examine a sample with a deliberately rough interface in order to enhance k. This was achieved by flashing the oxide off the substrate at a temperature greater than 530 °C. Under such circumstances, gallium droplets nucleate and the sample displays macroscopic roughness which manifests as an apparent "haze." This was sample 7, and it shows neither enhanced interface mode intensities nor frequency shifts which lie significantly outside the range of data obtained on samples known by x-ray analysis to be pseudomorphic. Were it not for the fact that similar results have been reported for the nearly lattice-matched GaAs/AlAs system,[9] one might have argued that interface strains in the present system represent a critical and as yet unaccounted for aspect of the problem. It would rather appear that our understanding of interface vibrations in these structures is somewhat incomplete.

C. Anomalous structure

Two sets of unanticipated scattering peaks labeled $S1$ and $S2$ in the figures were identified in the previous sections. We now consider the properties of these peaks and suggest possible assignments for their origins.

The structure $S1$ is relatively broad with two discernible peaks at ~ 211 and 218 cm^{-1}. (The peak frequencies have been downshifted by ~ 3.3 cm^{-1} to give 300 K values for subsequent comparison with phonon density of states calculations.) This structure is only observed in samples for which the GaSb layer width d_1 lies in the range $13.1 < d_1 < 31.2$ Å, and then only at liquid-nitrogen temperatures. All other samples including two (samples 1 and 5) with $d_1 \sim 50$ Å failed to exhibit $S1$-like peaks. This structure shows very little polarization dependence, even in the (x',y') configuration which normally attenuates all but the symmetry forbidden TO. The peaks are observed for both (001) and (111) growth orientations (see Fig. 7) if $d_1 \leq 32$ Å.

The d_1 layer thickness dependence for observation of $S1$ correlates quite closely with the size-induced Γ to L energy-gap transition previously reported in GaSb/AlSb quantum wells.[31,32] GaSb/AlSb superlattices display Type I electronic behavior (both electrons and holes are confined to the GaSb well layer) due to the fact that both the conduction and valence band offsets are large.[33–36] Since the Γ and L edges in GaSb are only separated by 80–90 meV and have very different subband electron masses, the GaSb quantum wells are expected to undergo a direct-to-indirect gap transition below some critical well width. This transition occurs for values of d_1 less than 30–40 Å,[32] and will result in a substantial population of electrons at the L point in photoexcited p-type samples at low temperatures.

The two peaks located within $S1$ at ~ 211 and 218 cm^{-1} (300 K) lie close to some of the recorded zone-boundary phonons at various critical points (primarily X,L) in the Brillouin zone of GaSb. This observation suggests that large wave-vector scattering processes become operative during the size-induced Γ to L gap transition in GaSb, and that one should examine the density of one-phonon states for structure consistent with that found in $S1$. In Fig. 10 we plot a scaled version of the calculated density of one-phonon states from Ref. 22 along with the observed form of $S1$. Since the second-order Γ_1 Raman spectrum (frequency scaled by a factor of 2) represents a weighted version of the density of phonon states, we have also included the data of Klein and Chang[37] in Fig. 10. The correlation between the second-order Raman spectrum and $S1$ is quite reasonable, although neither of the aforementioned spectra is in particularly good agreement with the calculated density of one-phonon states. This discrepancy has been attributed by the authors of Ref. 37 to the choice of the shell model parameters utilized in the calculation. The available evidence thus strongly suggests that $S1$ has its origin in large wave-vector scattering processes which replicate a weighted version of the phonon density of states.

The mechanism by which large wave vector scattering becomes activated *in first order* is not obvious. The most commonly encountered processes which break the momentum conservation condition typically entail defects in the form of impurities, nonstoichiometry, inho-

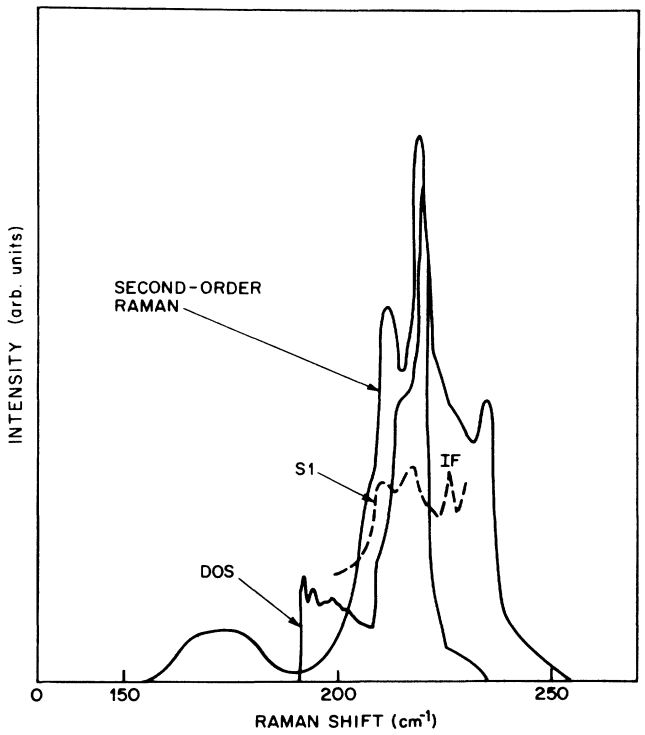

FIG. 10. Comparison of the room-temperature optical-phonon density of states for GaSb (Ref. 22) with the observed structure $S1$ and the (frequency shifted) second-order Raman spectrum of Ref. 37. The data for the $S1$ structure has been shifted ~ 3.3 cm^{-1} from its 77 K values in order to facilitate comparison. The peak denoted by IF is an interface mode.

mogeneities, or short-range order (amorphous or glassy materials). Strong optical absorption which certainly occurs in this system can also contribute to relaxation of momentum conservation. None of these mechanisms, however, are consistent with the observation that we only observe the structure $S1$ when the GaSb layers are sufficiently thin to induce a transition from a direct gap at Γ to an indirect gap at L. The correlation of $S1$ with the Γ to L transition indicates a strong dependence on the exact details of the electronic band structure in the superlattice and suggests consideration of resonance phenomena.

Resonance Raman scattering near critical points has been considered theoretically in detail by Martin[38] and Cardona.[39] Excitation at 5145 Å lies between the E_1 and $E_1+\Delta_1$ transitions in bulk GaSb, and a number of experimental studies for excitation at these transitions have been reported by Chang and co-workers.[40,41] They have observed a Fano-type Raman lineshape for resonant excitation at the E_1 and $E_1+\Delta_1$ gaps of GaSb and attributed it to coherent interactions between single-particle excitations of carriers located at Γ and large wave-vector LO phonons.[41] Unlike the present situation, they do not observe a phonon density-of-states–like structure between 200–220 cm^{-1}. The latter feature appears to be uniquely associated with the Γ to L energy-gap conversion. Additional resonance Raman studies in superlattice structures are required in order to elucidate the dominant scattering processes.

The properties of the peak labeled $S2$ which lies ~ 5.7 cm^{-1} below the AlSb TO frequency for (001)-oriented growth and ~ 7.4 cm^{-1} on (111) are distinct from those of $S1$. This peak has been observed on every sample at both 300 and 77 K independent of the values for d_1 and d_2. It displays polarization properties which are similar to the allowed m odd LO phonons (B_2 symmetry). We have observed this peak for scattering at 4880 Å, but with 6471 Å excitation (300 K), its intensity is reduced but not totally extinguished. The data at 6471 Å were taken in a pure backscattering configuration with a Raman microscope whose numerical aperture was 0.9. A comparison of the Raman signals taken at 5145 and 6471 Å is shown in Fig. 11.

There is no correlation between $S2$ and the size-induced direct-to-indirect gap transition which occurs in the GaSb well. One cannot discount near-resonance, large wave-vector scattering processes however, because both the E_0 (2.30 eV) and E_L (2.21 eV) gaps in AlSb are close to resonance with 5145 Å (2.41 eV) excitation. It is unlikely however, that $S2$ represents large wave-vector scattering leading to density-of-states–like structure. Recent calculations by Kagaya and Soma[42] indicate that the optic-mode dispersion in the (001) and (111) directions is relatively flat, and that the zone-boundary optic phonons at X and L lie at slightly higher frequencies than the TO at Γ. One therefore would not expect a peak 5–7 cm^{-1} *lower* than the TO(Γ) frequency if $S2$ were associated with scattering processes which generate a modulated version of the phonon density of optic modes.

The room-temperature frequency (~ 313 cm^{-1}) for $S2$ corresponds closely to the local mode frequency (~ 312.8 cm^{-1}) determined for Al in GaSb.[43] The polarization characteristics are also those of an LO phonon with B_2 symmetry. Since our superlattices are composed of the pure binary components, the assignment of $S2$ as a localized vibration for Al in GaSb implicitly presumes the existence of some interdiffusion. We observe no evidence for the Ga local mode in AlSb however, which should occur at ~ 205 cm^{-1} and be distinguished in samples where the $S1$ structure is absent. It is difficult to comment on the wavelength dependence since neither 5145 nor 6471 Å excitation is closely in resonance with the E_1 or $E_1+\Delta_1$ transitions in GaSb. For a localized mode in the GaSb layer, those would presumably be the relevant resonance transitions rather than the E_0 or E_L transitions in AlSb. The latter transitions would presumably affect the (unobserved) Ga local mode in AlSb. In our opinion, the assignment of $S2$ remains tenuous.

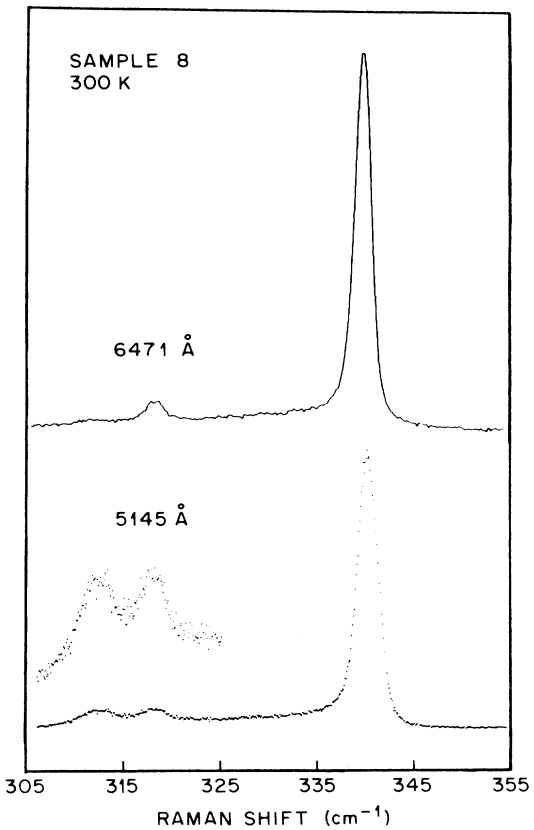

FIG. 11. Raman scattering from sample 8 at 300 K using 6471 (upper) and 5145 Å (lower) excitation.

IV. CONCLUSIONS

Raman scattering measurements have observed quantum confined and interface-mode optical phonons in strained-layer GaSb/AlSb superlattices. Optical-phonon confinement was observed in GaSb layers with thickness $d_1 < 25$ Å. Due to uncertainties in both the present experimental measurements and previous neutron

diffraction studies, it is not possible to state conclusively that the quantized LO phonon frequencies lie above the bulk dispersion curve for large wave vectors. Interface modes were detected in all samples independent of the period. The measured and calculated frequencies do not agree for any reasonable choice of wave vector for a backscattering geometry. This observation is not unique to strained-layer superlattices since similar results have been reported for the GaAs/AlAs system which is nearly lattice matched.

The size-induced Γ to L energy gap transition in the GaSb wells manifests itself in our data via large wave-vector scattering processes which result in structure similar to the optical phonon density of states. We also observe a peak lying 5–7 cm^{-1} below the TO(Γ) of AlSb which is tentatively assigned to local mode for Al in GaSb. We see no evidence however for Ga local modes in AlSb.

ACKNOWLEDGMENTS

During the course of this work it came to our attention that similar measurements have been pursued by Dr. A. K. Sood and Professor M. Cardona. One of us (G.P.S.) wishes to thank Dr. Sood for extensive discussions of the GaSb/AlSb system.

[1]A. S. Barker, Jr., J. L. Merz, and A. C. Gossard, Phys. Rev. B **17**, 3181 (1978).
[2]S.-K. Yip and Y.-C. Chang, Phys. Rev. B **12**, 7037 (1984).
[3]B. Djafari-Rouhani, J. Sapriel, and F. Bonnouvrier, Superlatt. Microstruct. **1**, 29 (1985).
[4]M. Babiker, J. Phys. C **19**, L339 (1986).
[5]R. Merlin, C. Colvard, M. V. Klein, H. Morkoc, A. Y. Cho, and A. C. Gossard, Appl. Phys. Lett. **36**, 43 (1980).
[6]J. Sapriel, J. C. Michel, J. C. Toledano, R. Vacher, J. Kervarec, and A. Regreny, Phys. Rev. B **28**, 2007 (1983).
[7]B. Jusserand, D. Paquet, and A. Regreny, Phys. Rev. B **30**, 6245 (1984).
[8]C. Colvard, T. A. Gant, M. V. Klein, R. Merlin, R. Fisher, H. Morkoc, and A. C. Gossard, Phys. Rev. B **31**, 2080 (1985).
[9]A. K. Sood, J. Menendez, M. Cardona, and K. Ploog, Phys. Rev. Lett. **54**, 2111 (1985).
[10]M. Nakayama, K. Kubota, T. Kanata, H. Kato, S. Chika, and N. Sano, Jpn. J. Appl. Phys. **24**, 1331 (1985).
[11]G. Kanellis, J. F. Morhange, and M. Balkanski, Phys. Rev. B **28**, 3406 (1983).
[12]E. Molinari, A. Fasolino, and K. Kunc, Phys. Rev. Lett. **56**, 1751 (1986).
[13]B. Jusserand and D. Paquet, Phys. Rev. Lett. **56**, 1752 (1986).
[14]E. P. Pokatilov and S. I. Beril, Phys. Status Solidi B **110**, KT5 (1982).
[15]E. P. Pokatilov and S. I. Beril, Phys. Status Solidi B **118**, 567 (1983).
[16]R. Lassnig, Phys. Rev. B **30**, 7132 (1984).
[17]A. K. Sood, J. Menendez, M. Cardona, and K. Ploog, Phys. Rev. Lett. **54**, 2115 (1985).
[18]G. P. Schwartz, G. J. Gualtieri, W. A. Sunder, L. A. Farrow, D. E. Aspnes, and A. A. Studna, J. Vac. Sci. Technol. A **5**, 1500 (1987).
[19]C. Colvard, R. Fisher, T. A. Grant, M. V. Klein, R. Merlin, H. Morkoc, and A. C. Gossard, Superlatt. Microstruct. **1**, 81 (1985).
[20]B. Jusserand, D. Paquet, and A. Regreny, Superlatt. Microstruct. **1**, 61 (1985).
[21]C. Alibert, A. Joullie, A. M. Joullie, and C. Ance, Phys. Rev. B **27**, 4946 (1983).
[22]M. K. Farr, J. G. Traylor, and S. K. Sinha, Phys. Rev. B **11**, 1587 (1975).
[23]A. K. Sood, J. Menendez, M. Cardona, and K. Ploog, Phys. Rev. Lett. **56**, 1753 (1986).
[24]P. B. Klein and R. K. Chang, Phys. Rev. B **14**, 2498 (1976).
[25]B. Jusserand, P. Voisin, M. Voos, L. L. Chang, E. E. Mendez, and L. Esaki, Appl. Phys. Lett. **46**, 678 (1985).
[26]S. M. Rytov, Sov. Phys. Acoust. **2**, 67 (1956).
[27]R. Fuchs and K. L. Kliewer, Phys. Rev. **140**, A2076 (1965).
[28]R. E. Camley and D. L. Mills, Phys. Rev. B **29**, 1695 (1984).
[29]R. Lassnig, Phys. Rev. B **30**, 7132 (1984).
[30]The value of 2000 Å is only approximate based on a limited set of x-ray and transmission-electron-microscopy data. Work is currently in progress to refine the critical thickness for GaSb/AlSb superlattices.
[31]g. Griffiths, K. Mohammed, S. Subbanna, H. Kroemer, and J. L. Merz, Appl. Phys. Lett. **43**, 1059 (1983).
[32]A. Forchel, U. Cebulla, G. Tränkle, H. Kroemer, S. Subbanna, and G. Griffiths, Surf. Sci. **174**, 143 (1986).
[33]G. J. Gualtieri, G. P. Schwartz, R. G. Nuzzo, and W. A. Sunder, Appl. Phys. Lett. **49**, 1037 (1986).
[34]E. E. Mendez, C. A. Chang, H. Takaoka, L. L. Chang, and L. Esaki, J. Vac. Sci. Technol. B **1**, 152 (1983).
[35]C. Tejedor, J. M. Calleja, F. Meseguer, E. E. Mendez, C. A. Chang, and L. Esaki, Phys. Rev. B **32**, 5303 (1985).
[36]F. Cerdeira, A. Pinczuk, T. H. Chiu, and W. T. Tsang, Phys. Rev. B **32**, 1390 (1985).
[37]P. B. Klein and R. K. Chang, Phys. Rev. B **14**, 2498 (1976).
[38]R. M. Martin, Phys. Rev. B **10**, 2620 (1974).
[39]M. Cardona, in *Light Scattering in Solids II*, edited by M. Cardona and G. Güntherodt (Springer-Verlag, New York, 1982), Chap. 2.
[40]R. L. Farrow and R. K. Chang, Solid-State Electron. **21**, 1347 (1978).
[41]R. Dornhaus, R. L. Farrow, and R. K. Chang, Solid State Commun. **35**, 123 (1980).
[42]H. M. Kagaya and T. Soma, Phys. Status Solidi B **127**, 89 (1985).
[43]G. Lucovsky, K. Y. Cheng, and G. L. Pearson, Phys. Rev. B **12**, 4135 (1975).